

## Determination of the just suspended speed for solid particle in torus reactor

Ali Alouache, Ammar Selatnia, Abdelouhab Lefkir, Farid Halet, Houssef Eddine Sayah and Boubekeur Nadjemi

### ABSTRACT

With the considerable use of pipelines and reactors in the engineering industry, determining the deposition velocity enabling hydraulic transport is of utmost importance. This has been investigated throughout the years, scrupulously in several types of reactors used in water treatment and solid transport. The primary focus has been extended to torus reactors, due to their significant advantage in chemical, biochemical and mixing processes. In the present work, we have studied the solid-liquid suspension in a torus reactor. We elaborated an experimental method based on visual assessment SBAM (Steady Bed Angle Method), which enabled us to analytically determine the just suspended speed 'N<sub>js</sub>' at which no solid remains stationary at the bed and further parametrically study the effect of several parameters including solid loadings, particle sizes and densities. The just suspended speed values obtained experimentally have been compared to a modified Zwietering's correlation.

**Key words** | agitation, just suspended speed, solid transportation, suspension, torus reactor

**Ali Alouache** (corresponding author)

**Ammar Selatnia**

**Farid Halet**

**Boubekeur Nadjemi**

Department of Chemistry,  
Laboratory of Study and Development of  
Techniques of Treatment and Water Treatment  
and Environmental Management L.E.D.T.E.G.E,  
E.N.S Kouba,

Algiers,

Algeria

E-mail: [alouacheali@yahoo.fr](mailto:alouacheali@yahoo.fr)

**Ammar Selatnia**

Department of Chemical Engineering,

National Polytechnic School E.N.P,

Algiers,

Algeria

**Abdelouhab Lefkir**

LTPITE Laboratory,

National School of Public Works (ENSTP),

Algiers,

Algeria

**Farid Halet**

**Houssef Eddine Sayah**

Faculty of Engineering Sciences,

M'Hamed Bougara University of Boumerdes

U.M.B.B,

Algeria

### NOMENCLATURE

N	Rotation speed (rpm)	$\varphi$	Pitched angle of impeller blade (deg)
N <sub>js</sub>	The just suspended speed (rpm)	D <sub>t</sub>	Inner diameter of pipe/torus reactor (m)
S <sub>v</sub>	Geometry coefficient (non dimensional)	R <sub>t</sub>	External radius of reactor (m)
$\rho$	Liquid density (kg/m <sup>3</sup> )	L <sub>t</sub>	Circumference length of reactor (m)
$\Delta\rho$	Density difference (kg/m <sup>3</sup> )	d <sub>2</sub>	Impeller axe diameter (m)
C <sub>v</sub>	Solid mass concentration (%)	$\rho_s$	Solid density (kg/m <sup>3</sup> )
D	Tank diameter	$\rho_l$	Liquid density (kg/m <sup>3</sup> )
v <sub>d</sub>	Deposing velocity (m/s)	$\alpha_0$	Maximum bed angle (deg)
F <sub>L</sub>	Froude criterion (non dimensional)	R	Ratio of bed angle (non dimensional)
d <sub>p</sub>	Average particle diameter (m)	SBAM	Steady Bed Angle Method
d <sub>1</sub>	Impeller diameter (m)	$\beta_1, \beta_2, \beta_3$	Constants
N	Rotation speed (rpm)	$\alpha_1, \alpha_2, \alpha_3$	Constants
v	Fluid velocity (m/s)	N <sub>jsSim</sub>	Simulated just suspended speed (rpm)

$N_{js_{Obs}}$	Observed just suspended speed (rpm)
$N_{js_{Obs}}^i$	Observed just suspended speed for the $i^{\text{th}}$ experience (rpm)
$N_{js_{Sim}}^i$	Simulated just suspended speed for the $i^{\text{th}}$ experience (rpm)
$\overline{N_{js_{Obs}}}$	Observed average just suspended speed (rpm)
$\overline{N_{js_{Sim}}}$	Simulated average just suspended speed (rpm)
$\sigma_{Obs}$	Standard deviation of measured $N_{js}$

## INTRODUCTION

Stirred reactors are widely used in industrial processes for heterogeneous chemical reactions and wastewater treatment; this type of reactor requires working at low stirring speed, causing solid particles to deposit on reactor walls, limiting both mass and heat transfer.

For this exact reason, manufacturers recommend increasing the agitation speed to reach the complete suspension necessary for solid-liquid transport. At values lower than the just suspended speed,  $N_{js}$ , the solid-liquid exchange surface is partial with some particles remaining stationary at the bottom of the reactor, some suspended, and a few denominated as jumping particles. This leads to a decrease in mass and heat transfer crucial to some solid-liquid operations for the completion of the reaction in a heterogeneous mixture according to Cohen *et al.* (2018). Contrarily, at values superior to the just suspended speed  $N_{js}$ , the solid-liquid mass-transfer is inconsequential, it is of note that all particles in this case possess the same concentration. Hence, we observe a significant drop in productivity and an unnecessary power consumption. In order to hinder this problem, researchers focused on determining the minimal suspension speed. Davoody *et al.* (2015) worked on maximizing the particle interfacial area while also minimizing the agitation cost. In addition, Tamburini *et al.* (2016b) were able to effectively augment the solid loading per reactor unit volume while keeping the operation costs as low as possible.

Zwietering (1958), Nienow (1968) and Baldi *et al.* (1977) studied back in the 1950s and 1970s the dependence of the critical speed ( $N_{js}$ ) on physical and geometrical parameters of the reactor and the operating conditions.

A slight effort has been devoted to investigating solid-liquid suspension in unbaffled stirred tanks, used preferably for wetting and drawing down particles into liquids. The issue of solid particles suspension in this kind of reactor

was tackled for the very first time by Brucato *et al.* (2010). In order to avoid vortex formation and dead volume at high stirring speed, they opted for a cover on top of the tank. A significant mass transfer coefficient was observed in unbaffled tanks compared to baffled ones, for the same power dissipation and a difference of density between solid and liquid phases. Moreover, turbulence is generally predominant in unbaffled tanks due to excellent heat and mass transfer, improving the chemical reaction according to Li *et al.* (2015). Tamburini *et al.* (2015) also observed a significant power saving when using the unbaffled tank, for processes where the mixing time is not a limiting factor.

The stirred tank and pipe have been fully explored in the study of solid-liquid mixing with many studies carried out experimentally to determine the just suspended speed for complete suspension (Taghavi *et al.* 2014). The minimum liquid velocity necessary to prevent deposition of solids of horizontal pipes in hydraulic transport of sand and water has been investigated by Durand (1952).

Taghavi *et al.* (2014) designed a new mixing mechanism for conventional stirred tank reactors, improving its mixing characteristics.

Limited research has been devoted to solid-liquid suspension in loop reactor, tackled for the very first time in slurry polymerization of olefins. This type of reactor has potential applications in both biochemical reactions and processing of highly viscous liquids According to Sato *et al.* (1979); Murakami *et al.* (1982); and Nouri *et al.* (1997), it presents various advantages such as the prevention of polymer deposition at high Reynolds number and a heat transfer area per unit of reactor volume larger than stirred tank reactors. To proceed toward bulk polymerization of olefins, the loop reactor is operated at high Reynolds number in order to prevent polymer deposition, this leads to an increase in power consumption that must be taken into account for the design and operation of the reactor according to Murakami *et al.* (1982). For polymer suspension, adhesion of polymer on reactor walls ought to be prevented. Laederach & Widmer (1984) recommended an intensive mixing in order to ensure homogeneous distribution of phases and a full-on suspension of micro-organisms. At high impeller speed, no decrease of hydrolysis of wheat proteins was observed, as reported by Nouri *et al.* (1997) and Nasrallah *et al.* (2008), who stated that the main flow and mixing influencing parameters were the rotating speed, diameter and type of impeller.

According to Laederach & Widmer (1984), micro-organisms often tend to deposit in thick layers on the walls of the reactor, resulting in the depletion of active organisms in the reaction solution and a significant drop

in productivity and/or product quality mainly because the organisms forming the layer are subject to a substrate limitation. Therefore, they suggested a high recirculation frequency, which has the effect of increasing the power dissipated by the stirrer.

Almost all researchers recommend working at high Reynolds number (high agitation speed) in order to prevent solid particles' deposition at the reactor walls and impeller (Sato *et al.* 1979; Murakami *et al.* 1982; Laederach & Widmer 1984; Tanaka *et al.* 1989). The minimal rotational speed at which all the solid particles were to be suspended has never been determined in a torus reactor.

The aim of this work is to experimentally determine the just suspended speed ( $N_{js}$ ) in a torus reactor, comparing it to a modified Zwietering's correlation calculated value. A parametric study of the  $N_{js}$  has also been conducted (concentration, particles size, density). An experimental method based on visualization (Steady Bed Angle Method, SBAM) was elaborated to identify  $N_{js}$  in a torus reactor.

## MATERIALS AND METHODS

### Theoretical approach

Some efforts have been directed towards estimating the value of  $N_{js}$  using theoretical models; however, not all of these models can be considered as universally applicable. Most of these are solely based on the distinction between suspended and non-suspended particles. Tamburini *et al.* (2016a) in their work identified the complete suspension conditions. Zwietering back in the 1950s studied the suspension of particles and considered them completely suspended if they did not remain stationary at the bottom of the pipe or the reactor more than 1 s.

Several works were performed throughout the years to determine experimentally the just suspended speed  $N_{js}$  in stirred reactors, with many researchers applying various correlations and models to best describe the phenomena of suspension. Brucato *et al.* (2010) have used Equation (1), first proposed by Zwietering (1958) for standard baffled vessels, presented as follows:

$$N_{js} = \frac{S_v^{0.1} d_p^{0.2} (\Delta\rho/\rho)^{0.45} C_v^{0.13}}{D^{0.85}} \quad (1)$$

where  $N_{js}$  is the just suspended agitation speed (rpm),  $S_v$  the geometry coefficient (non dimensional),  $d_p$  the particle diameter (m),  $\Delta\rho$  the density difference between solid

particles and liquid ( $\text{kg/m}^3$ ),  $C_v$  the weight of the solid in suspension per weight of liquid, times 100 (non dimensional) and  $D$ , the tank diameter (m).

Representing the lowest velocity at which slurry pipelines would be able to operate, the minimal deposition speed is crucial, and therefore ought to be evaluated. This velocity is largely dependent on solid concentration, particle density and size as well as pipe diameter according to Kaushal *et al.* (2002). A large number of correlations have been prompted by researchers to predict the deposition velocity in pipes, most of which are commonly based on the Froude criterion, with a limited range of applicability for hydraulic transport of sand and water slurries in horizontal pipes (Kaushal *et al.* 2002). For hydraulic transport of sand and water slurries in horizontal pipes, Durand (1952) investigated the minimal liquid velocity required to prevent deposition of solids based on uniform size particles, proposing a correlation as follows:

$$v_d = F_L [2gD(\Delta\rho/\rho)]^{1/2} \quad (2)$$

where  $v_d$  is the depositing velocity (m/s). Wasp *et al.* (1977) have compared the Durand correlation given by Equation (2) with data from Durand (1952) and Wicks (1968) to predict the deposition velocity of sand and water slurries. They concluded that the Durand correlation gives excellent prediction with an exception for low solids concentration (1% by volume). Wasp *et al.* (1977) modified Equation (2) for the deposition velocity of high concentrations in fully turbulent flow based on Wicks (1968) as follows:

$$v_d = 4 \left( \frac{d_p}{D_t} \right)^{1/6} (C_v)^{1/5} [2gD(\Delta\rho/\rho)]^{1/2} \quad (3)$$

In the loop reactor, Sato *et al.* (1979) have given the link between the mean fluid velocity ( $v$ ) and the rotation speed ( $N$ ) of the marine screw impeller and it is represented as follows:

$$v = \pi N \left( \frac{d_1}{2} \right) \sin\varphi \quad (4)$$

where  $v$  is the fluid velocity (m/s),  $d_1$  the impeller diameter (m), and  $\varphi$  the pitched angle of the impeller blade (deg). According to Zwietering (1958) and Nienow (1968), Equation (1) could be used to calculate  $N_{js}$  in a tank reactor. Wasp *et al.* (1977) and Kaushal *et al.* (2002) have used Equations (2) and (3) to estimate the deposition velocity in horizontal pipes. The just suspended speed ( $N_{js}$ ) in a torus

reactor can be calculated by combining Equation (3) proposed by Wasp et al. (1977) and Equation (4) proposed by Sato et al. (1979). The combined form of these equations allowed us to lay a modified version of Zwietering's correlation, which is expressed as follows:

$$N_{js} = \frac{4(d_p/D_t)^{1/6} (C_v)^{1/5} [2gD(\Delta\rho/\rho)]^{1/2}}{\pi(d_1/2)\sin\varphi} \quad (5)$$

### Validation criterion

The model was validated using two methods: a graphical method, using correlation curves and a statistical method using validation criteria. Simulated results were compared to experimental (observed) data. Two criteria were adopted for this study.

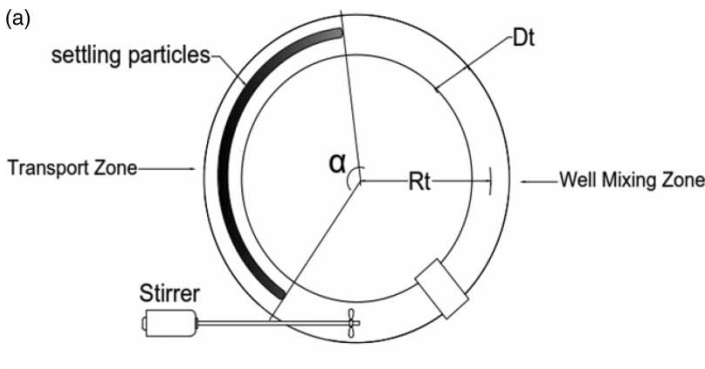
The determination coefficient ( $R^2$ ) assesses the relationship between the observed and simulated values; it is expressed as follows (Maachou et al. 2017):

$$R^2 = \frac{\sum_{i=1}^n ((Njs_{Obs}^i - \overline{Njs}_{Obs})(Njs_{Sim}^i - \overline{Njs}_{Sim}))}{\sum_{i=1}^n (Njs_{Obs}^i - \overline{Njs}_{Obs})^2 \times \sum_{i=1}^n (Njs_{Sim}^i - \overline{Njs}_{Sim})^2} \quad (6)$$

where  $Njs_{Obs}^i$  represents the measured value of Njs for the  $i^{\text{th}}$  experience and  $Njs_{Sim}^i$  the simulated value.

**Table 1** | General performance ratings for recommended statistical criteria

Rating	RSR (%)	R <sup>2</sup> (%)
Very good	0 ≤ RSR ≤ 50	75 < R <sup>2</sup> ≤ 100
Good	50 < RSR ≤ 60	65 < R <sup>2</sup> ≤ 75
Satisfactory	60 < RSR ≤ 70	50 < R <sup>2</sup> ≤ 65
Unsatisfactory	RSR > 70	R <sup>2</sup> ≤ 50



$\overline{Njs}_{Obs}$  and  $\overline{Njs}_{Sim}$  represent respectively the measured and simulated average rate with  $n$ , the number of experiences.

Root Mean Square Error (RMSE) is used to measure the distortion between the observed and simulated values. RMSE is expressed as follows:

$$RMSE = \sqrt{\frac{1}{n} \sum_{i=1}^{n_{obs}} (Njs_{Sim}^i - Njs_{Obs}^i)^2} \quad (7)$$

RSR: is a dimensionless quantity that expresses the dispersion between simulated and observed values and defined as the RMSE Standard-Deviation Ratio.

$$RSR(\%) = 100 \cdot \frac{RMSE}{\sigma_{Obs}} = 100 \cdot \frac{\sqrt{\sum_{i=1}^{n_{obs}} (Njs_{Sim}^i - Njs_{Obs}^i)^2}}{\sqrt{\sum_{i=1}^{n_{obs}} (Njs_{Obs}^i - \overline{Njs}_{Obs})^2}} \quad (8)$$

where  $\sigma_{Obs}$  represents the standard deviation of measured Njs. RSR varies from zero, which indicates a low residual variability and therefore perfect model simulation, to a positive value. Table 1 shows the values of RSR and  $R^2$  criteria corresponding to different degrees of performance of the model (Khemissi et al. 2019).

### Description of the experimental device

The torus reactor used in this study and presented in Figure 1 is similar to that used by researchers (Belleville et al. 1992; Nouri et al. 2008; Nasrallah et al. 2008). Our device has been built using transparent pipes of inner diameter ( $D_t$ ) of 50 mm, and a circumference length of 1,400 mm, which corresponds to a total volume of 2.9 L as shown in

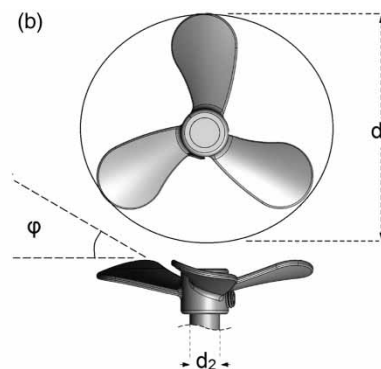


**Figure 1** | Schematic of the torus reactor. (a) Description of settling bed. (b) The marine screw impeller.

**Table 2** | Characteristics of the torus reactor and the marine screw impeller

Torus reactor	$D_t$ (mm)	$L_t$ (mm)	$R_t$ (mm)
	50	1,600	250
Marine screw impeller	$d_1$ (mm)	$d_2$ (mm)	$\Phi$
	40	6	45°

Figure 1(a). The mixing was achieved by a marine screw impeller as shown in Figure 1(b). The stirring was driven by a variable speed motor (IKA-WERK RW20).

This type of reactor has been formerly used in wastewater treatment by Alouache et al. (2017), geometrical characteristics of both the torus reactor and the marine screw impeller are given in Table 2.

### Measurement techniques and procedure

A large number of researchers have focused on the study of the just suspended speed for particles suspension, with the assessment based on experimental visualization (Armenante et al. 1992; Legrand 2007; Kuzmani et al. 2008; Brucato et al. 2010; Jirout & Rieger 2010; Ravelet et al. 2013). For this reason (Brucato et al. 2010) proposed an experimental method (the Steady Cone Radius Method, SCRM) in order to determine ( $N_{js}$ ) in stirred tank reactor. According to (Zwietering 1958) for new systems such as in our case, the torus reactor, new experimental trials would be more accurate.

The experiment has been performed using transparent torus reactor fixed upon a table made of glass under which a mirror is accurately placed to capture its bottom. Only visual observations were made, no samples were taken from the suspension vessel, a simple digital camera was used for images acquisition. Solid particles of different materials and size were tested in water solution. The characteristics of solid particles are presented in Table 3.

In the present case, and for ( $N_{js}$ ) measurement, an experimental method (Steady Bed Angle Method)

**Table 3** | Characteristics of solid particles

Material	$d_p$ ( $\mu\text{m}$ )	Average $d_p$ ( $\mu\text{m}$ )	$\rho_s$ ( $\text{kg}/\text{m}^3$ )
Sand	160–315	237.5	2,400
	315–450	357.5	
	400–500	450	
Siporex	315–450	357.5	1,900
Biomass	50–160	105	1,200
	200–250	225	
	400–500	450	

based on visualization was elaborated and enabled us to identify the just suspended conditions in torus reactor as illustrated in Figure 2(a). The solid particles were introduced into the reactor, followed by an additional amount of water until reaching the reactor's volume.

The reactor is agitated at a high speed, permitting a homogeneous distribution of solid particles, after which the engine is stopped, leading to a precipitation of all the particles along the circumference reactor bottom, forming a particles settling bed with an angle  $\alpha_0 = 360^\circ$  as shown in Figure 2(b).

By gradually increasing the stirring speed, the solid particles in the vicinity of the marine screw impeller are suspended, causing the decrease of the bed length of solid particles deposited at the reactor bottom. The angle formed between the two ends of the bed is measured by a protractor as shown in Figure 2(c) and 2(d). The camera is installed above the reactor; allowing visualization of the reflected image of the reactor bottom by the mirror placed below the reactor.

The choice of placing the camera above the reactor is aimed at: a better acquisition of the image of the reactor bottom; avoid that the support of the camera would be an obstacle for taking pictures.

The images taken by the camera are transmitted and visualized on a computer thus making it possible to manually adjust accurately the needles placed on both ends of the bed formed by the solid particles deposited at the reactor bottom. The angle  $\alpha$  measurement is made between the bed boundaries, it was taken with agitation and until a stable bed was formed.

For each solid concentration the just suspended speed ( $N_{js}$ ) is determined by varying agitation speed from 200 rpm until the speed at which the settling bed disappears, it corresponds to ( $\alpha = 0^\circ$ ). For each value of the stirring speed  $N$ , we obtain a certain angle  $\alpha$  to calculate the ratio  $R$  as a function of  $N$  (rpm) for each concentration ( $C_v$ ) of the solid particles. The increase in agitation speed leads to a decrease in the angle formed by the settling bed from  $\alpha_0 = 360^\circ$  (partial suspension) to  $\alpha = 0^\circ$  (complete suspension). The ratio  $R$  presented in Equation (9) can be exploited to determine the agitation speed at which no particles remain steady on the reactor bottom (complete suspension), this corresponds to ( $R = 0$ ). And according to (Zwietering 1958) it corresponds to no particles remaining stationary at the bottom of the reactor more than 1 s.

$$R = \frac{\alpha}{\alpha_0} \quad (9)$$

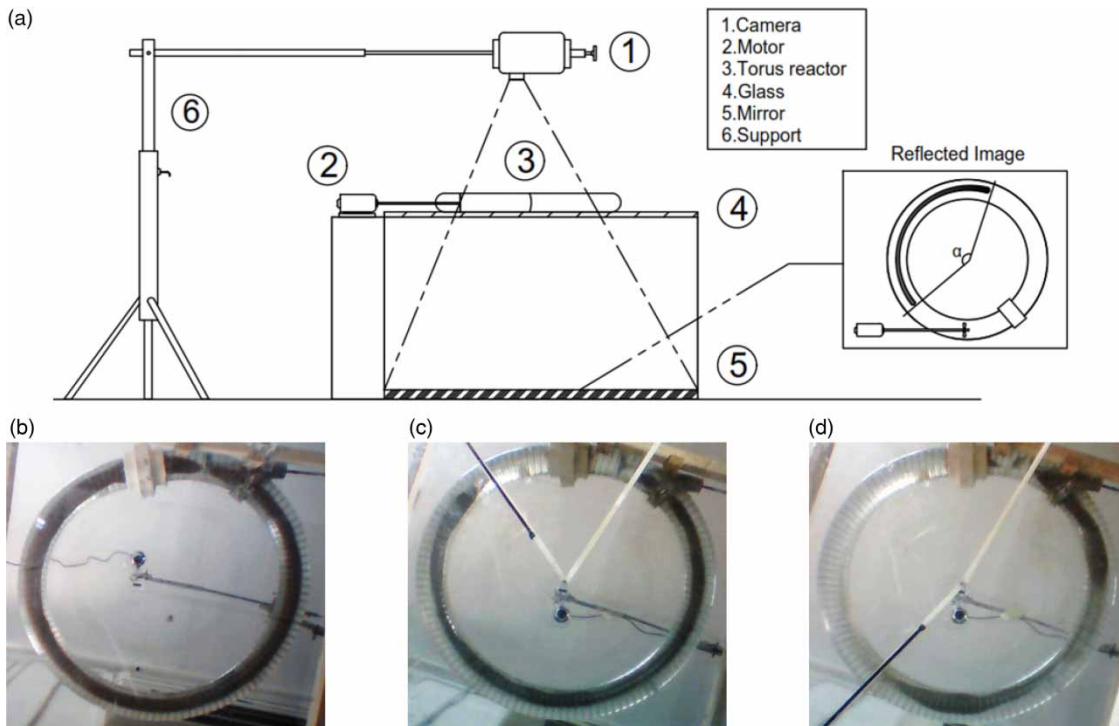


**Figure 2** | Njs measurement (SBAM) apparatus: (a) global schemas of measurement device, (b) settling bed, (c) partial suspension (low speed), (d) partial suspension (high speed).

Figure 3 shows the plot of  $R$  according to  $N$  for different solid particles concentration  $C_v$  in the reactor. For low values of the stirring speed ( $N$ ) of less than 300 rpm, the ratio  $R$  tends to 1, which indicates that the bed formed by the solid particles remain almost stable throughout the bottom of the reactor. When increasing the stirring speed,

the angle  $\alpha$  decreases to the point where its visual measurement becomes difficult. The plot of the experimental points has a polynomial shape, its extrapolation towards the abscissa axis makes it possible to reach the value of the ratio  $R=0$  which corresponds to the angle  $\alpha=0$ , where there will be no more solid particles deposited on the reactor

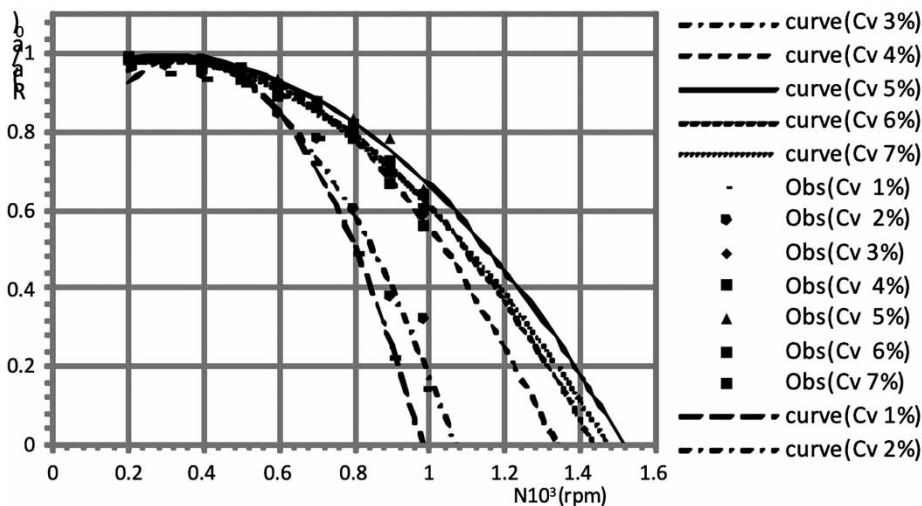


**Figure 3** | Njs determination.

bottom for more than 1 to 2 s (Zweitering). The stirring speed at this point represents the just suspended speed ( $N_{js}$ ) computed by second-order polynomial interpolation. All experiments were performed at least twice.

The SBAM method has the advantage of avoiding measurement subjectivity and gives excellent reproducibility. Same remarks were observed by (Brucato et al. 2010) in stirred tank reactor.

The well mixed zone contains suspended particles in opposite of the transport zone which corresponds to the bed formed by the settling and jumped particles.

At the just suspended speed ( $N_{js}$ ), the volume of the transport zone tends to zero which corresponds to  $\alpha = 0^\circ$ , the torus reactor would then be composed only by the well mixed zone. As a result, an improvement of the mixture is obtained. The hydrodynamics of the fluid depend on the characteristics of solid particles, liquid phase, reactor geometry and the stirring parameters, which affect the suspension of these solid particles in the solution (Taghavi et al. 2014).

In torus reactor experiments, the suspension phenomenon can be explained by the existence of two zones as illustrated in Figure 1(a). A well-mixed zone as in case of a constant stirred tank reactor upstream and downstream the impeller, and a transport zone as in case of a plug flow. There is a boundary existing between the two zones contained in the torus volume. When a variation of agitation speed occurs, not only the volumes of the zones vary but their location within the torus evolves counter-clockwise (Dieulot et al. 2005). For a positive variation in impeller speed, the volume of the well-mixed zone increases whereas that of the transport zone decreases.

## RESULTS AND DISCUSSION

### Effect of particle concentration

For different sizes of sand particles, the dependence of  $N_{js}$  on solid mass concentration ( $C_v$ ) is illustrated in Figure 4(a). In the same figure and for comparison purposes, lines reporting the  $N_{js}$  values for all particle sizes calculated by Equation (5) are reported. It can be seen that increasing ( $C_v$ ) increases the required ( $N_{js}$ ) to remove the settling bed and keep all particles suspended.

For small sand diameters, it was found that the majority of the observed  $N_{js}$  values (experimental) are contained in the two theoretical envelope curves resulting from Equation (5). Taking into account  $R^2$  and RSR, the best results for these criteria: ( $R^2 > 92\%$ ) and RSR (RSR = 53%) are obtained for small sand particle sizes ( $d_p = 237.5 \mu\text{m}$ ), see Table 3. The ( $N_{js}$ ) dependence on particle concentration in the torus reactor is similar compared to that given by Equation (5)  $N_{JS} = \alpha_1 C_v^{\beta_1}$  where ( $\beta_1 = 0.2$ ). The criteria used to validate the model are shown in Table 4.

**Table 4** | Validation criteria of simulated model for different  $d_p$  with  $C_v$  as a variable

	Biomass			Sand		
	$R^2$ (%)	RMSE (rpm)	RSR (%)	$R^2$	RMSE (rpm)	RSR (%)
$d_p = 105 \mu\text{m}$	91.19	160.97	54	/	/	/
$d_p = 225 \mu\text{m}$	0.02	32.02	211	/	/	/
$d_p = 237,5 \mu\text{m}$	/	/	/	92.08	210.94	53
$d_p = 355.5 \mu\text{m}$	/	/	/	92.39	32.04	248
$d_p = 450 \mu\text{m}$	42.13	70.36	58	15.81	64.32	347

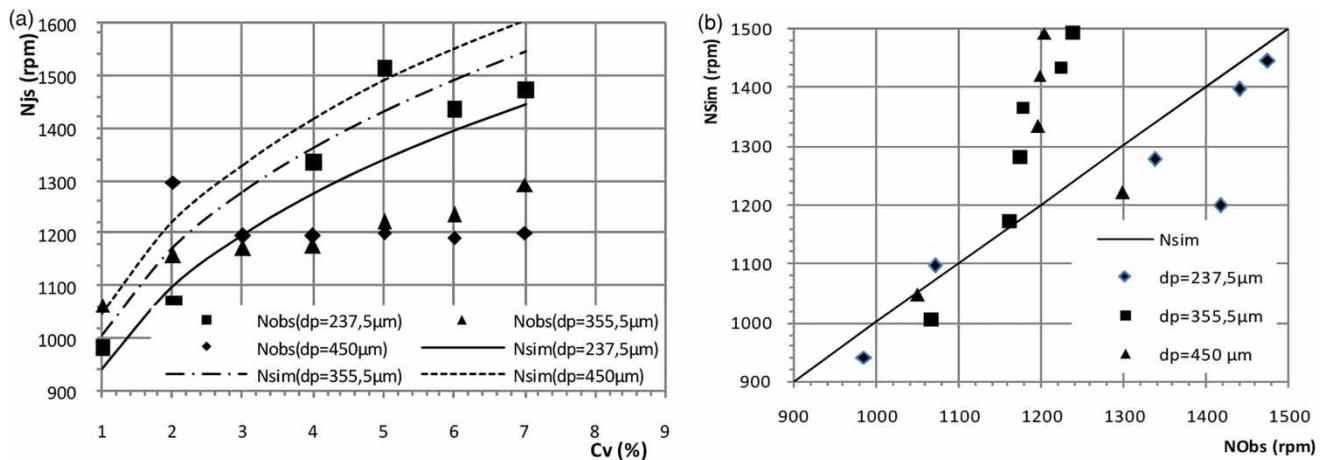


**Figure 4** | (a) Dependence of  $N_{js}$  on particles concentration of sand for different particle size. (b) Correlation curve of observed  $N_{js}$  (NObs) and simulated  $N_{js}$  (NSim) of sand for different particle size.

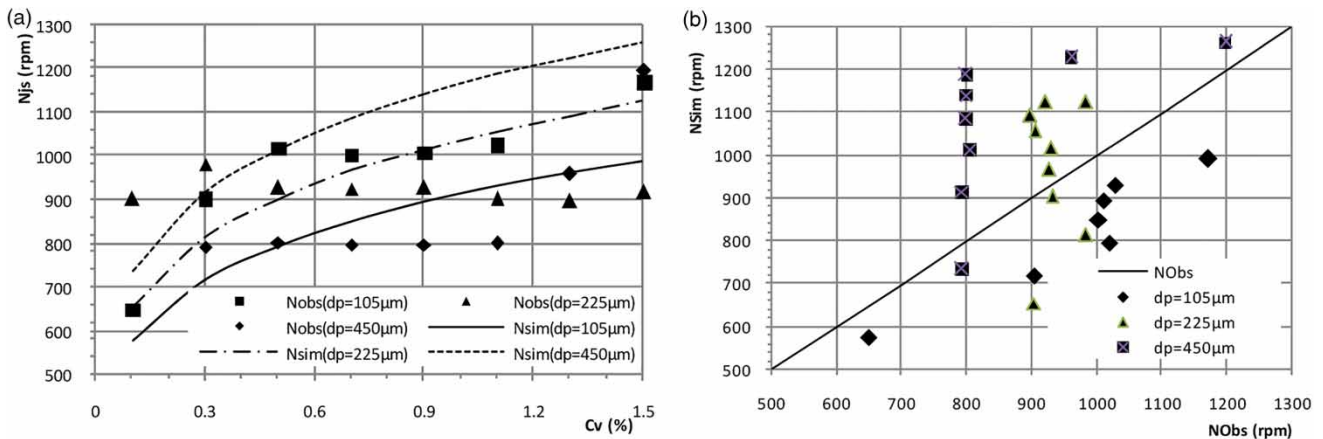


**Figure 5** | (a) Dependence of  $N_{js}$  on particles concentration of biomass for different particle size. (b) Correlation plot of observed  $N_{js}$  (NObs) and simulated  $N_{js}$  (NSim) of biomass for different particle size.

However, for large diameters 355 and 450  $\mu\text{m}$ , Unsatisfactory results have been obtained, these results are illustrated in the correlation curve showed in Figure 4(b), where there is an overestimation of  $N_{js}$  simulated by the Equation (5).

To apply these results in wastewater treatment, we have studied a solid particle widely used in this field, named '*Pleurotus mutilus* biomass', used in small portions in order to remove toxic components of low concentrations.  $N_{js}$  was tested for low biomass concentrations as illustrated in Figure 5(a). It can be seen that for different particles concentration investigated.  $N_{js}$  values ranged between 800 and 1,000 (rpm).

For biomass, proceeding similarly to sand particles described above. It can be seen that the theoretical model gives a very good values for smaller particle diameters ( $d_p = 105 \mu\text{m}$ ), with ( $R^2 > 91\%$ ) and ( $RSR = 54\%$ ). However, the model cannot simulate large diameters. This observation was verified graphically by the correlation curve shown in

Figure 5(b). Indeed the model overestimates the values of  $N_{js}$  for large values of  $d_p$ .

### Effect of particle size

According to the experimental tests carried out in the laboratory on the range of selected granulometry, we found that the suspension speed  $N_{js}$  decreases with the increase in particle size. The  $N_{js}$  values presented in Figure 6(a) are plotted as a function of particle size  $d_p$ . In the same figure are reported the calculated values of  $N_{js}$  for sand particles using Equation (5) for low concentration (solid line) and high concentration (dotted line) validated later on with the experimental results. It is found that the majority of the values of the  $N_{js}$  given experimentally are contained in the two theoretical envelope curves resulting from Equation (5). The validation criteria given in Table 5 show a very good appreciation of the theoretical model

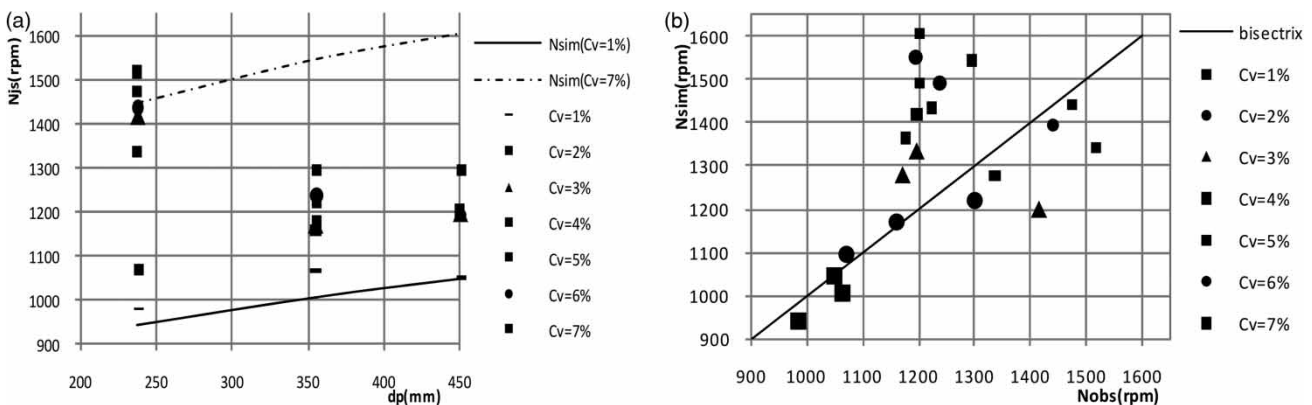


**Figure 6** | (a) Dependence of  $N_{js}$  on particle size of sand for different concentrations. (b) Correlation plot of observed  $N_{js}$  (NObs) and simulated  $N_{js}$  (NSim) of sand for different concentrations.



**Table 5** | Validation criteria of simulated model for different concentrations with  $d_p$  as a variable

	Cv = 1%	Cv = 2%	Cv = 3%	Cv = 4%	Cv = 5%	Cv = 6%	Cv = 7%
R <sup>2</sup> (%)	70.65	93.44	79.20	76.61	89.34	95.22	99.75
RMSE (rpm)	41.78	48.71	161.40	172.38	230.28	255.94	274.68
RSR (%)	57.60	42.33	120.12	197.86	131.02	195.70	199.49

with R<sup>2</sup> values range (71–99%); however, good appreciations of RSR values are obtained for low values of Cv (1%, 2%).

For the small diameters range and for the low solid concentrations, we found a slight difference between experimental results and simulated ones of the proposed correlation, which could be representative. For low solid concentration, and low  $d_p$  the (N<sub>js</sub>) dependence on particle size in the torus reactor is similar to that given by Equation (5)  $N_{js} = \alpha_2 d_p^{\beta_2}$  where ( $\beta_2 = 1/6$ ).

The correlation curves given in Figure 6(b) confirm the previous observation that of an overestimation of N<sub>js</sub> for larger values of C<sub>v</sub>.

For the range of particle size investigated here, It can be seen that the dependence of N<sub>js</sub> is much smaller for large particle sizes, and the correlation is no longer applicable, similar results were observed by Brucato. An increase in particle size has little effect on the N<sub>js</sub> value; according to these results one may ideally think to use the largest particle size without increasing the stirring speed necessary to have complete suspension. The extrapolation of these results outside the size range investigated in this study presents risks and cannot be extended to large particle sizes. The same remarks were presented by (Brucato et al. 2010) in stirred tank reactor.

We noticed the decrease in N<sub>js</sub> with the increase of particle sizes. As a matter of fact, the fine particles develop a larger contact area and thus greater shear stresses, (Westerholm et al. 2008; Chang & Powell 2013) whereas for large particle sizes, we notice the exact opposite. The detachment of small particles requires a greater inertia

force. Thus a higher N<sub>js</sub> speed, which justifies the surprising experimental values found.

### Effect of particle density

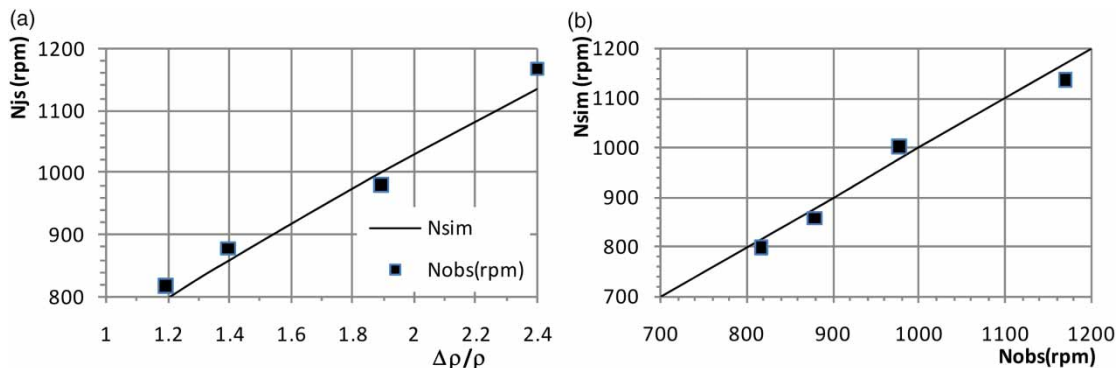
Different types of solid have been studied such as: sand, siporex, and biomass. Figure 7(a) represents (N<sub>js</sub>) plotted as a function of  $\Delta\rho/\rho$ , the (N<sub>js</sub>) is largely dependent on the difference in relative density between solid particles and liquid. We note that the higher density increases the rotational speed limit N<sub>js</sub> necessary to get complete suspension in solution within the limits of experimental errors. Therefore, the density has the same impact as the concentration of solid particles.

The (N<sub>js</sub>) dependence on liquid/solid relative density difference in the torus reactor is similar to that given by Equation (5)  $N_{js} = \alpha_3 (\Delta\rho/\rho)^{\beta_3}$  where ( $\beta_3 = 1/2$ ).

According to the curves of Figure 7(a) and 7(b), a perfect correlation is observed between the measured values of N<sub>js</sub> and the simulated ones, with a very appreciable values of R<sup>2</sup> (97.41%) and RSR (16%).

### CONCLUSION

Experiments in solid-liquid suspension for the torus reactor were performed. A new experimental method (Steady Bed Angle Method, SBAM) based on visualization has been

**Figure 7** | (a) Dependence of N<sub>js</sub> on relative particle density difference. (b) Correlation curve of observed N<sub>js</sub> (NOBs) and simulated N<sub>js</sub> (Nsim) for different particle density of solids.

elaborated to enable the visual assessment of the just suspended speed  $N_{js}$ .

We have studied various solid particles widely used in wastewater treatment and chemical reaction (biomass, sand). For each solid concentration, we have determined the just suspended speed ( $N_{js}$ ), above which mass and heat transfer are inconsequential. This explains some kinetic reaction where mass transfer is a limiting factor.

The parameters affecting  $N_{js}$ , such as particle concentration, particle diameter and particle density, were investigated and compared with that calculated by our modified Zwietering's correlation. Similarity between experimental and theoretical values has been noted for the just suspended speed ( $N_{js}$ ) for particle concentration and density difference.

It seems that the suspended speed in a torus reactor is proportional to the concentration and particle density and particle size, noting that the dependence on the particle diameter is negligible for large particle size. Deducing that our results are quite similar to researchers, the correlations give a good agreement for low concentration and small diameters.

For future research in torus reactor, these results can be exploited to ensure a homogeneous solution in wastewater treatment, and expand research toward optimization of speed values to avoid solid deposition and increase mass and heat transfer.

This type of reactor has promising applications in solid transportation and wastewater treatment. It can be suggested that it should be in continuous mode to facilitate its industrial application. The research results indicate that accurate calculation of the minimal velocity necessary for complete suspension could serve as an efficient method for solid-liquid mixing. This study is expected to lead to further research on suspension for different types of solid particles used in the engineering industry, as well as the geometric and physical parameters that affect the just suspended speed while also reducing costs of operations.

## ACKNOWLEDGEMENTS

The authors are thankful to Aoudia Cherif, engineer at Eurl ANFM Bordj el Bahri Algiers for building the reactor and its accessories.

## REFERENCES

Alouache, A., Selatnia, A. & Halet, F. 2017 Biosorption of Cr (VI) from aqueous solutions by dead biomass of *Pleurotus*

*mutilus* in torus reactor. In: *Frontiers in Wastewater Treatment and Modelling (FICWTM)* (G. Mannina, ed.). Springer, Cham, Switzerland.

- Armenante, P. M., Huang, Y.-T. & T, L. I. 1992 Determination of the minimum agitation speed to attain the just dispersed state in solid-liquid and liquid-liquid reactors provided with multiple impellers. *Chemical Engineering Science* **47** (9), 2865–2870.
- Baldi, G., Conti, R. & Alaria, E. 1977 Complete suspension of particles in mechanically agitated vessels. *Chemical Engineering Science* **33** (1), 21–25.
- Belleville, P., Nouri, L. & Legrand, J. 1992 Mixing characteristics in the torus reactor. *Chemical Engineering Technology* **15**, 282–289.
- Brucato, A., Cipollina, A., Micale, G., Scargiali, F. & Tamburini, A. 2010 Particle suspension in top-covered unbaffled tanks. *Chemical Engineering Science* **65** (10), 3001–3008.
- Chang, C. & Powell, R. L. 2013 Effect of particle size distributions on the rheology of concentrated bimodal suspensions of concentrated bimodal suspensions. *Journal of Rheology* **85** (1994), 85–98.
- Cohen, B. M., Inankur, B., Lauser, K. T., Lott, J. & Chen, W. 2018 Evaluation of just-suspended speed correlations in lab-scale tanks with varying baffle configurations. *Organic Process Research & Development* **22** (1), 1481–1488.
- Davoody, M., Aziz, A., Abdul, B. & Parthasarathy, R. 2015 Maximizing impeller power efficiency in gas – solid – liquid stirred vessels through process intensification. *Industrial and Engineering Chemistry Research* **54**, 11915–11928.
- Dieulot, J., Petit, N., Rouchon, P. & Delaplace, G. 2005 An arrangement of ideal zones with shifting boundaries as a way to model mixing processes in unsteady stirring conditions in agitated vessels. *Chemical Engineering Science* **60**, 5544–5554.
- Durand, R. 1952 The hydraulic transport of coal and other materials in pipe, Paper IV. In: *The Proceedings of Colloquium on Hydraulic Transportation of Coal*. London, UK, pp. 39–52.
- Jirout, T. & Rieger, F. 2010 Impeller design for mixing of suspensions. *Chemical Engineering Research and Design* **89**, 1144–1151.
- Kaushal, D. R., Tomita, Y. & Dighade, R. R. 2002 Concentration at the pipe bottom at deposition velocity for transportation of commercial slurries through pipeline. *Powder Technology* **125**, 89–101.
- Khemissi, H., Hartani, T., Remini, B., Lefkir, A., Abda, L. & Heddami, S. 2019 A hybrid model for modelling the salinity of the Tafna River in Algeria. *Journal Of Water And Land Development* **40** (1), 127–135.
- Kuzmani, N., Zaneti, R. & Akrap, M. 2008 Impact of floating suspended solids on the homogenisation of the liquid phase in dual-impeller agitated vessel. *Chemical Engineering and Processing* **47**, 663–669.
- Laederach, H. & Widmer, F. 1984 Le bioreacteur torique. *Information Chimie* **249**, 157–160.

- Legrand, A. 2007 **Characterization of solid–liquid suspensions (real, large non-spherical particles in non-Newtonian carrier fluid) flowing in horizontal and vertical pipes.** *Journal of Food Engineering* **78**, 345–355.
- Li, J., Deng, B., Zhang, B., Shen, X. & Kim, C. N. 2015 **CFD simulation of an unbaffled stirred tank reactor driven by a magnetic rod: assessment of turbulence models.** *Water Science & Technology* **72**, 1308–1318.
- Maachou, R., Lefkir, A., Bermad, A., Djaoui, T. & Khouider, A. 2017 **Statistical analysis of pollution parameters in activated sludge process.** *Desalination and Water Treatment* **72**, 85–91.
- Murakami, Y., Hirose, T., Ono, S., Eitoku, H. & Nishijima, T. 1982 **Power consumption and pumping characteristics in a loop reactor.** *Industrial and Engineering Chemistry Process Design and Development* **21** (2), 273–276.
- Nasrallah, N., Legrand, J., Bensmaili, A. & Nouri, L. 2008 **Effect of impeller type on the mixing in torus reactors.** *Chemical Engineering and Processing* **47**, 2175–2183.
- Nienow, A. W. 1968 **Suspension of solid particles in turbine agitated baffled vessels.** *Chemical Engineering Science* **23**, 1453–1459.
- Nouri, L., Legrand, J., Popineau, Y. & Belleville, P. 1997 **Enzymatic hydrolysis of wheat proteins Part 2: comparison of performance of batch-stirred and torus reactors.** *Chemical Engineering Journal* **65**, 195–199.
- Nouri, L., Legrand, J., Benmalek, N., Imerzoukene, F., Yeddou, A. & Halet, F. 2008 **Characterisation and comparison of the micromixing efficiency in torus and batch stirred reactors.** *Chemical Engineering Journal* **142**, 78–86.
- Ravelet, F., Bakir, F., Khelladi, S. & Rey, R. 2013 **Experimental study of hydraulic transport of large particles in horizontal pipes.** *Experimental Thermal and Fluid Science* **45**, 187–197.
- Sato, Y., Murakami, Y., Hirose, T., Hashigushi, Y., Ono, S. & Ichikawa, M. 1979 **Flow pattern, circulation velocity and pressure loss in loop reactor.** *J. Chem. Eng. Jpn* **12**, 448–453.
- Taghavi, M., Ebrahimi, S. & Moghaddas, J. 2014 **Solid particle distribution in centrifugal impeller contactors.** *Journal of Dispersion Science and Technology* **35** (8), 1097–1105.
- Tamburini, A., Cipollina, A., Grisafi, F., Scargiali, F., Micale, G. & Brucato, A. 2015 **Comparison of agitators performance for particle suspension in top-covered unbaffled vessels.** *Chemical Engineering Transactions* **43**, 1585–1590.
- Tamburini, A., Cipollina, A., Micale, G., Scargiali, F., Brucato, A., Chimica, I., Palermo, U. & Edi, S. 2016a **Particle suspension in vortexing unbaffled stirred tanks.** *Industrial and Engineering Chemistry Research* **55**, 7535–7547.
- Tamburini, A., Cipollina, A., Scargiali, F., Micale, G. & Brucato, A. 2016b **Power requirements for complete suspension and aeration in an unbaffled bioslurry reactor.** *Chemical Engineering Transactions* **49**, 451–456.
- Tanaka, M., Sendai, T. & Hosogai, K. 1989 **Flowing characteristics in a circular loop reactor.** *Chemical Engineering Research and Design* **67**, 423–427.
- Wasp, E., Kenny, J. & Gandhi, R. 1977 **Solid–liquid flow: slurry pipeline transportation. Pumps, valves, mechanical equipment, economics.** Trans Tech Publications, Clausthal, Germany.
- Westerholm, M., Silfwerbrand, J. & Forssberg, E. 2008 **Influence of fine aggregate characteristics on the rheological properties of mortars.** *Cement & Concrete Composites* **30**, 274–282.
- Wicks, M. 1968 **Transportation of solids at low concentration in horizontal pipes.** In: *ASCE INTL. Symposium on Solid-Liquid Flow in Pipe*. University of Pennsylvania, PA, USA.
- Zwietering, T. N. 1958 **Suspending of solid particles in liquid by agitators.** *Chemical Engineering Science* **8** (3–4), 244–253.

First received 12 February 2019; accepted in revised form 9 July 2019. Available online 22 July 2019